Effects and potential mechanism of Ca²⁺/calmodulin-dependent protein kinase II pathway inhibitor KN93 on the development of ovarian follicle

JIANJIE YU[1,2], XIANGUO XIE[1], YABO MA[1], YI YANG[1], CHAO WANG[1,3], GUOLIANG XIA[1,3], XIANGBIN DING[2] and XINFENG LIU[1]

[1]Key Laboratory of Ministry of Education for Conservation and Utilization of Special Biological Resources in Western China, College of Life Science, Ningxia University, Yinchuan, Ningxia Hui Autonomous Region 750021; [2]Tianjin Key Laboratory of Agricultural Animal Breeding and Healthy Husbandry, College of Animal Science and Veterinary Medicine, Tianjin Agricultural University, Tianjin 300384; [3]Department of Physiology, State Key Laboratory of Agrobiotechnology, College of Biological Sciences, China Agricultural University, Beijing 100193, P.R. China

Abstract. Adequate regulation of the speed of follicular development has been reported to prolong the reproductive life of the ovary. The aim of the present study was to assess the potential effects and mechanism of the Ca²⁺/calmodulin-dependent protein kinase II (CaMKII) pathway on the development of ovarian follicle. In the present study, the expression of CaMKII was measured in the ovary of mice at different developmental stages by immunofluorescence, confirming that CaMKII has a role in follicular development. Subsequently, the 17.5 days post-coitus (dpc) embryonic ovaries were collected and cultured with KN93 for 4 days *in vitro*. It was revealed that KN93 inhibited the development of follicles, where it reduced the expression levels of oocyte and granulosa cell markers DEAD-box helicase 4 (DDX4) and forkhead box L2 (FOXL2). These results suggested that KN93 could delay follicular development. Proteomics technology was then used to find that 262 proteins of KN93 treated 17.5 dpc embryonic ovaries were significantly altered after *in vitro* culture. Bioinformatics analysis was used to analyze these altered proteins. In total, four important Kyoto Encyclopedia of Genes and Genome pathways, namely steroid biosynthesis, p53 signaling pathway and retinol metabolism and metabolic pathways, were particularly enriched. Further analysis revealed that the upregulated proteins NADP-dependent steroid dehydrogenase-like (Nsdhl),

lanosterol synthase (Lss), farnesyl-diphosphate farnesyltransferase 1 (Fdft1), cytochrome P450 family 51 family A member 1 (Cyp51a1), hydroxymethylglutaryl-CoA synthase 1 (Hmgcs1), fatty acid synthase (Fasn) and dimethylallyltranstransferase (Fdps) were directly interacting with each other in the four enriched pathways. In summary, the potential mechanism of KN93 in slowing down follicular development most likely lies in its inhibitory effects on CaMKII, which upregulated the expression of Nsdhl, Lss, Fdft1, Cyp51a1, Hmgcs1, Fasn and Fdps. This downregulated the expression of oocyte and granulosa cell markers DDX4 and FOXL2 in the follicles, thereby delaying follicular development. Overall, these results provide novel insight into the potential mechanism by which KN93 and CaMKII can delay follicular development.

Introduction

Follicles form the basic reproductive unit of female mammalians and are important not only for ovulation, but also for the production of hormones that maintain the secondary sexual characteristics and early pregnancy (1). According to the previously reported morphological and functional changes that occur during follicular development, follicles can be divided into primordial, primary, secondary and mature follicles (2-4). In particular, formation and activation of primordial follicles is key for determining reproductive ability (5). In the majority of mammalian species, the formation of primordial follicles typically occurs during the embryonic stages or around birth (6-8). By contrast, in adult ovaries, primordial follicles cannot be renewed and regenerated (6-8). Therefore, the size of the primordial follicle pool is mainly used to determine the reproductive capacity of female mammals throughout their lifetime (6-8).

The primordial follicle is comprised of an immature oocyte and several flattened precursor granulosa cells wrapped around it. After the primordial follicle becomes activated to form a primary follicle, it then consists of an oocyte along with one or several layers of cubic granulosa cells wrapped around

Correspondence to: Dr Xinfeng Liu, Key Laboratory of Ministry of Education for Conservation and Utilization of Special Biological Resources in Western China, College of Life Science, Ningxia University, 489 Helan Mountain West Road, Xixia, Yinchuan, Ningxia Hui Autonomous Region 750021, P.R. China
E-mail: liu2019074@nxu.edu.cn

it. At present, a number of studies have been performed on the formation and activation of primordial follicles, which mainly reported the involvement of various signaling pathways, including Notch, PI3K, Janus kinase, TGF-β and KIT (9-13). However, the mechanism underling primordial follicle formation and activation remains poorly understood.

Calmodulin-dependent protein kinase (CaMK) serves an important role in reproductive regulation. CaMK belongs to the serine/threonine kinase family and consists of four members, namely CaMK I, II, IV and K, where CaMKII is the most widely studied (14-16). CaMKII is a 8-12 polymer and is comprised of four homologous genes CaMKIIA, CaMKIIB, CaMKIIG and CaMKIID, along with their corresponding expression products CaMKIIα, CaMKIIβ, CaMKIIγ and CaMKIIδ (17). Previous studies have demonstrated that CaMKII is closely associated with the activation of oocytes, where ~80% of MII-phase mouse oocytes with CaMKIIγ expression knocked down can be activated after the overexpression of CaMKIIγ or CaMKIIδ (18). CaMKII also serves an important role in the development of early mouse embryos. It has been previously revealed that the expression of CaMKIIγ can be detected in mouse embryos in the two-celled stage, where it can regulate the development of these embryos by regulating the activation levels of cAMP response element-binding protein and cAMP-dependent transcription factor (19). Although these findings suggest that CaMKII can serve an important role in reproductive regulation, the effect of CaMKII on follicular development remains unknown.

KN93 is a CaM-binding specific antagonist that can reversibly and competitively inhibit CaMKII activity (20,21). Several studies have previously reported that KN93 can affect physiological and pathological processes in the body by inhibiting CaMKII, including the brain, nervous system, cardiovascular system and cancer (22-25). Combined with previous reports, it is likely that CaMKII serves an important role in reproductive regulation. However, to the best of our knowledge, the effects of KN93 as a specific inhibitor of CaMKII on follicular development remain to be reported.

In mice, the embryonic females from 17.5 days post-coitus (dpc) is the initial stage of primordial follicular formation, whereas the neonatal females from 5 days post-partum (dpp) is the stage of primordial follicular bank formation. For this reason, in the present study, the expression levels of CaMKII in the ovaries of mice at different development stages (17.5, 1, 3 and 5 dpp) were measured using immunofluorescence. It was revealed that the expression of CaMKII was obviously changed in ovary of mice at the various developmental stages. Therefore, it was hypothesized that CaMKII has a potential role in regulating follicular development. Based on this, KN93 was selected to inhibit CaMKII to study the possible role and potential mechanism of KN93 in regulating follicular development after inhibiting CaMKII.

Materials and methods

Animal and ovary collection. ICR mice were selected for the present study because of their high fecundity characteristics. Adult ICR mice, 10 males and 60 females (8-10 weeks old; male, 34-38 g; female, 24-28 g), were purchased from Beijing Vital River Laboratory Animal Technology Co., Ltd. All

mice were housed in an environment with 50±10% humidity, lighting (12-h light/dark cycle) and temperature (24-26°C) conditions with free access to food and water. Animal experiments were approved by the Animal Ethical and Welfare Committee of Ningxia University (approval no. IACUC-N DLAC-2020019). Mice health and behavior were monitored daily. No mouse death occurred during the experiment. The total cumulative duration of the experiment was 8 months, excluding some time gaps.

All female mice were randomly divided into four groups as follows: 17.5 dpc Embryonic ovaries group (45 mice), 1 dpp neonatal ovaries group (five mice), 3 dpp neonatal ovaries group (five mice) and 5 dpp neonatal ovaries group (five mice). These female mice were randomly assigned in batches to mate with adult males at a ratio of 1:1 overnight. Mice with a vaginal plug in the next morning were defined at 0.5 dpc. Whereas, mice without a vaginal plug were scheduled for another round of mating. The day after partum was considered to be 1 dpp. The mice at 17.5 days of pregnancy (45 mice) were euthanized by cervical dislocation. Following sacrifice, the abdomen was immediately cut open to obtain the fetuses *in utero*. These fetuses were also euthanized by cervical dislocation to collect embryonic ovaries (17.5 dpc). Additionally, female mice at 1, 3 and 5 days after birth (10 each) were randomly selected and euthanized by cervical dislocation to collect neonatal ovaries (1, 3 and 5 dpp). Mouse ovaries were separated in cold PBS under a stereo-microscope in sterile conditions. During this procedure, care was taken to ensure that the structure of the whole ovaries was not damaged. After the experiment, all remaining animals were euthanized by cervical dislocation. In the present study, all animal's mortalities were confirmed by determining the lack of heartbeat and respiration.

Ovary culture. The 17.5 dpc ovaries were cultured in six-well culture plates in 1,500 μl DMEM/Ham F12 nutrient mixture (Gibco; Thermo Fisher Scientific, Inc.) supplemented with insulin-transferrin-sodium selenite (1:100; Sigma-Aldrich; Merck KGaA) and 1% penicillin-streptomycin solution at 37°C, 5% CO_2 and saturated humidity. The mouse ovaries were randomly assigned so that there were the same number of ovaries in each group. The culture medium was exchanged once every 2 days. The different concentration (5, 10 and 10 μM) of KN93 (cat. no. S6787; Selleck Chemicals) was added in the treatment group. The control group was instead treated with an equivalent volume of DMSO. The ovaries were then cultured for 4 days to assess the role of KN93.

Hematoxylin staining. Ovaries were fixed in 4% paraformaldehyde at 4°C overnight, embedded in paraffin and sectioned serially at 5 μm. Sections were then adhered onto the slides and stained with hematoxylin at room temperature (12 sec) for detecting the presence of oocytes and follicles with the Nikon 80i digital fluorescence microscope (Nikon Corporation).

Immunofluorescence staining. Ovaries were fixed in 4% paraformaldehyde at 4°C overnight, embedded in paraffin and sectioned serially at 5 μm. The sections were deparaffinized at 60°C for 20 min and washed for 5 min with xylene (cat. no. 33535; Yantai Shuangshuang Chemical Co., Ltd.) twice. Then the sections were rehydrated in descending alcohol

(cat. no. 64-17-5; Tianjin Damao Chemical Reagent Factory) series and subjected to high temperature (95-98˚C) antigen retrieval in 0.01% sodium citrate buffer (pH 6.0). The sections were then rinsed thoroughly with PBS, blocked with normal donkey serum (cat. no. ZX108; Beijing Zoman Biotechnology Co.,Ltd.) in PBS for 1 h at room temperature and incubated with primary antibodies for 12-16 h at 4˚C. The antibodies used were as follows: Anti-CaMKII antibody (1:200; cat. no. ab52476; Abcam), DEAD-box helicase 4 (DDX4; 1:50; cat. no. ab27591; Abcam) and anti-forkhead box L2 (FOXL2) antibody (1:100; cat. no. NB100-1277; Novus Biologicals, LLC). Subsequently, the ovarian sections were rinsed thoroughly with PBS and incubated with Alexa Fluor 488 AffiniPure donkey anti-mouse IgG (H+L; 1:200; cat. no. 34106ES60; Shanghai Yeasen Biotechnology Co.,Ltd.) or Donkey anti-goat IgG (H+L) highly cross-adsorbed secondary antibody, Alexa Fluor™ Plus 555 (1:200; cat. no. A32816; Invitrogen; Thermo Fisher Scientific, Inc.) for 1 h at 37˚C. The slides were then rinsed in PBS, stained with Hoechst 33342 at 37˚C (1:1,000; cat. no. B2261; Sigma-Aldrich; Merck KGaA) for 5 min and sealed in the anti-fade fluorescence mounting medium (cat. no. 20180116; Applygen Technologies, Inc.) with coverslips. Sections were examined and images were captured using the Nikon 80i digital fluorescence microscope (Nikon Corporation).

Protein isolation, quantification digestion and desalting. The proteins were extracted from the ovary samples of control group and KN93 treatment group, and the Bradford method was used to determine protein concentration according to the previously described method (26). Proteins were reduced with 1 M DL-Dithiothreitol (DTT; cat. no. 3483-12-3; Beijing Solarbio Science & Technology Co., Ltd.) at 56˚C for 30 min, cooled to room temperature, alkylated with 0.55 M iodo-acetamide (cat. no. 144-48-9; Shanghai Aladdin Bio-chem Technology Co., Ltd.) in a darkroom for 30 min at room temperature and 10 mM DTT was added and precipitated at -20˚C for 2 h. The sample was centrifuged at 4˚C, 13,000 x g for 20 min and the supernatant discarded. Subsequently, 1 ml cold acetone (cat. no. 144-48-9; Sinopharm Chemical Reagent Co., Ltd.) was added to the precipitate to give a final concentration of 10 mM DTT. The precipitate was thoroughly mashed-up, vortexed and left to stand for 30 min at -20˚C, then centrifuged at 4˚C, 13,000 x g for 20 min and the supernatant discarded. The precipitate was air-dried, with 8 M Urea (cat. no. U5378; Sigma-Aldrich; Merck KGaA) lysis buffer was added and sonicated at 4˚C for 5 min (working 1 sec, stopping 2 sec), and then centrifuged at 4˚C, 13,000 x g for 20 min. The supernatant was collected and the Bradford method was used to determine protein concentration. The reduced and alkylated proteins were digested using trypsin (cat. no. V5111; Promega Corporation) in a volume ratio of 1:100 (enzyme/protein) at 37˚C for >8 h. A total of 10 mg of C18 column material was weighed, corresponding to every 100 μg of peptide sample. The column material was activated using 1 ml methanol (cat. no. 10014118; Sinopharm Chemical Reagent Co., Ltd.), centrifuged instantaneously with shaking at room temperature and the supernatant was discarded. Added 1 ml 0.1% formic acid (FA; cat. no. 80065518; Sinopharm Chemical Reagent Co., Ltd.) to acidify at room temperature for 30 sec, centrifuged instantaneously with shaking at room temperature and

discarded the supernatant. Peptide samples were acidified with an equal volume of 0.1% FA, shaken, vortexed into a centrifuge tube, mixed at room temperature for 30 min by muter mixer and centrifuged instantaneously with shaking at room temperature to discard the supernatant. The sample was then washed twice with 0.1% FA + 3% acetonitrile (ACN; cat. no. 40064193; Sinopharm Chemical Reagent Co., Ltd.) for desalting and eluted with 1 ml 0.1% FA + 80% ACN. The eluted peptide was dried with a vacuum concentrator.

HPLC-MS/MS analysis. The analysis was performed using QEXactive HF-X (Thermo Fisher Scientific, Inc) liquid mass spectrometry system. The samples were separated by a liquid phase UltiMate 3000 RSLCnano system (Thermo Fisher Scientific, Inc.) at a nanoliter flow rate. The peptide samples were dissolved by loading buffer, inhaled by automatic sampler and bound to C18 capture column (3 μm, 120 Å, 100 μm x 20 mm; Thermo Fisher Scientific, Inc), and then eluted to an analysis column (2 μm, 120 Å, 750 μm x 250 mm) for separation. An analytical gradient was established using two mobile phases (mobile phase A: 98% water, 2% ACN, 0.1% FA; and mobile phase B: 98% ACN, 2% water, 0.1% FA). The flow rate of the liquid phase was set at 300 nl/min. In the Data Dependent Acquisition (DDA) mode analysis of MS, each scan cycle contains a full MS scan (R=60 K; AGC=3e6; Max IT=20 MS; Scan range=350-1,800 m/z). And then 20 MS/MS scans (R=15 K; AGC=2e5; Max IT=100 MS). Electrospray ionization ion source ion type was positive ion, atomizer voltage was set to 2.2 kV, impact gas pressure was automatically optimized with sample type, nitrogen temperature (ion transfer tube temperature) was 320˚C, HCD impact energy was set to 28. The filter window for the quad pole was set to 1.6 DA. The dynamic exclusion time of ion repeated collection was set to 35 sec and raw data for mass detection (.raw) was generated.

Data analysis and bioinformatics analysis. The raw MS data obtained from three biological replicates were combined and imported into MaxQuant software (version 1.6.17.0; Max Planck Institute of Biochemistry) to identify and quantify the proteins. For protein identification, the MS data were aligned to the Uniport Mus_musculus protein database (Proteome ID: UP000000589; https://www.uniprot.org/proteomes/UP000000589) represented by the file uniport (PR1-21010013-PR1-21010015-uniprot-Mus_musculus-10090-v20210123.fasta). The MS/MS tolerance of first search with an error window of 20 ppm and then with a main search error of 4.5 ppm. The proteins were cleaved using trypsin, and the two missed cleavages were accepted. Peptide identifications with false discovery rates >1% were discarded. Proteins with an adjusted [log2 (fold-change)]>2 and P<0.05 or [log2 (fold-change)] <0.5 and P<0.05 were identified differentially expressed proteins. Gene Ontology (GO; http://www.geneontology.org/) annotations and Kyoto Encyclopedia of Genes and Genomes (KEGG; http://www.genome.jp/kegg/) metabolic pathway analyses were performed to identify possible enrichment of the differential expressed proteins with particular biological characteristics. Taking P-value ≤0.01 as the threshold, the GO terms or KEGG terms that meet this condition in the DEPs were called the enrichment GO terms

or KEGG terms. Furthermore, all interactions and network construction were performed in the STRING 11.0 database (http://string-db.org/).

Western blotting. Each protein sample was obtained from ≥ eight ovaries after extraction in the WIP Tissue and cell lysis solution containing 1 mM PMSF (cat. no. 8553S; Cell Signaling Technology, Inc.) according to the manufacturer's protocols. Protein concentration was measured using a BCA assay (cat. no. P0012; Beyotime Institute of Biotechnology). The samples (10 μg) were separated on 10% SDS-PAGE and then transferred onto PVDF membranes. The membranes were blocked with 5% skimmed milk powder for 1 h at room temperature. The membranes were then incubated overnight at 4˚C with the appropriate primary antibodies. CaMKII (1:300; cat. no. ab52476; Abcam), DDX4 (1:500; cat. no. ab27591; Abcam), FOXL2 (1:500; cat. no. NB100-1277; Novus Biologicals, LLC), cytochrome P450 family 51 family A member 1 (CYP51A1; 1:2,000; cat. no. 13431-1-AP; ProteinTech Group, Inc.), fas-associated death domain (FADD; 1:5,000; cat. no. ab124812; Abcam), neural cell adhesion molecule 1 (NCAM1; 1:1,000; cat. no. ab220360; Abcam), cytochrome *c*, testis (Cyct; 1:5,000; cat. no. ab133504; Abcam), insulin-like growth factor binding protein 3 (IGFBP3; 1:1,000; cat. no. ab220429; Abcam), plastin 1 (1:1,000; cat. no. A15303; ABclonal Biotech Co., Ltd.), PDZ domain-containing 1 (PDZK1; 1:5,000; cat. no. ab92491; Abcam), zona pellicida sperm-binding protein (ZP2; 1:2,000; cat. no. A10126; ABclonal Biotech Co., Ltd.), Y-box binding protein 2 (YBX2; 1:5000; cat. no. ab154829; Abcam) and Bcl-2-interacting protein 3-like (BNIP3L; 1:5,000; cat. no. ab109414; Abcam). After rinsing thoroughly with TBST, the membranes were incubated with secondary antibodies (1:5,000; cat. no. ZB-2301; ZSGB-BIO). The membranes were then visualized using SuperSignal West Pico chemiluminescent detection system (cat. no. 34080; Thermo Fisher Scientific, Inc.). GAPDH (1:1,000; cat. no. AF7021; Affinity Biosciences) was used as an intrinsic control. An ImageJ software (version 1.8.0; National Institutes of Health) was used to quantify the relative expression of each protein.

Statistical analysis. All experiments were repeated ≥3 times. The data were analyzed using unpaired Student's t-test by GraphPad Prism 8 (GraphPad Software, Inc.) and presented as the mean ± standard deviation (SD). P<0.05 was considered to indicate a statistically significant difference.

Results

Expression of CaMKII in the embryonic and neonatal mouse ovaries. To explore the potential role of CaMKII in follicular development, ovaries from 17.5 dpc embryonic mice and ovaries from 1, 3 and 5 dpp newborn mice were collected to prepare tissue sections. Immunofluorescence was first performed in the follicles to detect the localization and expression pattern of CaMKII at different developmental stages by co-staining CaMKII and the oocyte specific marker DDX4. The expression of CaMKII was detected in ovaries at different developmental stages. In particular, CaMKII was revealed to be mainly localized to the cytoplasm of ovarian granulosa

cells in embryonic and newborn mice (Fig. 1). It has been previously reported that the initial stage of primordial follicle formation in mouse ovaries is embryonic 17.5 dpc (27). In the present study, CaMKII was mainly expressed in the ovarian cortex of 17.5 dpc embryos, where only a small number of primordial follicles were revealed (Fig. 1). In the ovaries of neonatal 1 dpp mice, CaMKII expression extended from the cortex into the medulla region (Fig. 1), where more primordial follicles were revealed. In the ovaries of 3 and 5 dpp neonatal mice, primordial follicles were more extensively activated and developed into primary follicles. During these two stages of development, CaMKII was mainly expressed in the medulla region of the ovary and in the granulosa cell cytoplasm within the primordial and primary follicle (Fig. 1). These results suggested that CaMKII was involved in follicular development by regulating the function of granulosa cells, especially the formation or activation of primordial follicles.

KN93 inhibits CaMKII and delays follicular development. To study the effects of CaMKII on follicular development further, KN93, an inhibitor of CaMKII, was used in the present study. Different doses of KN93 (5, 10 and 15 μM) were selected to treat 17.5 dpc embryonic ovaries for 4 days *in vitro* before H&E staining to detect the progress of ovarian development. It was revealed that 5 μM exerted no notable effects on ovarian development, whilst 15 μM KN93 mediated marked influence on the development of the ovary but seriously damaged its structure. By contrast, the effects of 10 μM were relatively moderate, which not only exerted notable impact on the development of ovarian follicles but also induced relatively little damage to the ovarian tissue structure (Fig. S1). Therefore, 10 μM was selected as the final dose for subsequent experiments in the present study.

H&E staining also indicated that the development of follicles in the control group was markedly faster compared with that in the 10 and 15 μM KN93 treatment group. In addition, it was revealed that a large number of primordial follicles in the control group had migrated to the ovarian medulla region, which were activated and developed into primary follicles. However, no similar phenomenon was observed in the 10 and 15 μM KN93 treatment groups (Fig. S1).

Subsequently, western blotting revealed that KN93 could significantly inhibit CaMKII expression in addition to significantly reducing the expression of the oocyte specific marker DDX4 and the granulosa cell specific marker FOXL2 in follicles (Fig. 2). Immunofluorescence detection results validated the western blotting data, in that the fluorescence intensity of the oocyte marker DDX4 and the granulosa cell marker FOXL2 in the ovarian follicles from the KN93 treatment group was weaker compared with that in the control group (Fig. 3). In the enlarged view of the ovaries in the control group, a large number of primordial and primary follicles could be observed, whilst there are only a small number of primordial follicles in the KN93 group. This suggested that the development of follicles in the KN93 treatment group was inhibited, consistent with the results of hematoxylin staining (Fig. 3). These results suggested that KN93 downregulated the expression of the oocyte marker DDX4 and the granulosa cell marker FOXL2 in follicles by inhibiting CaMKII, thereby delaying follicular development.
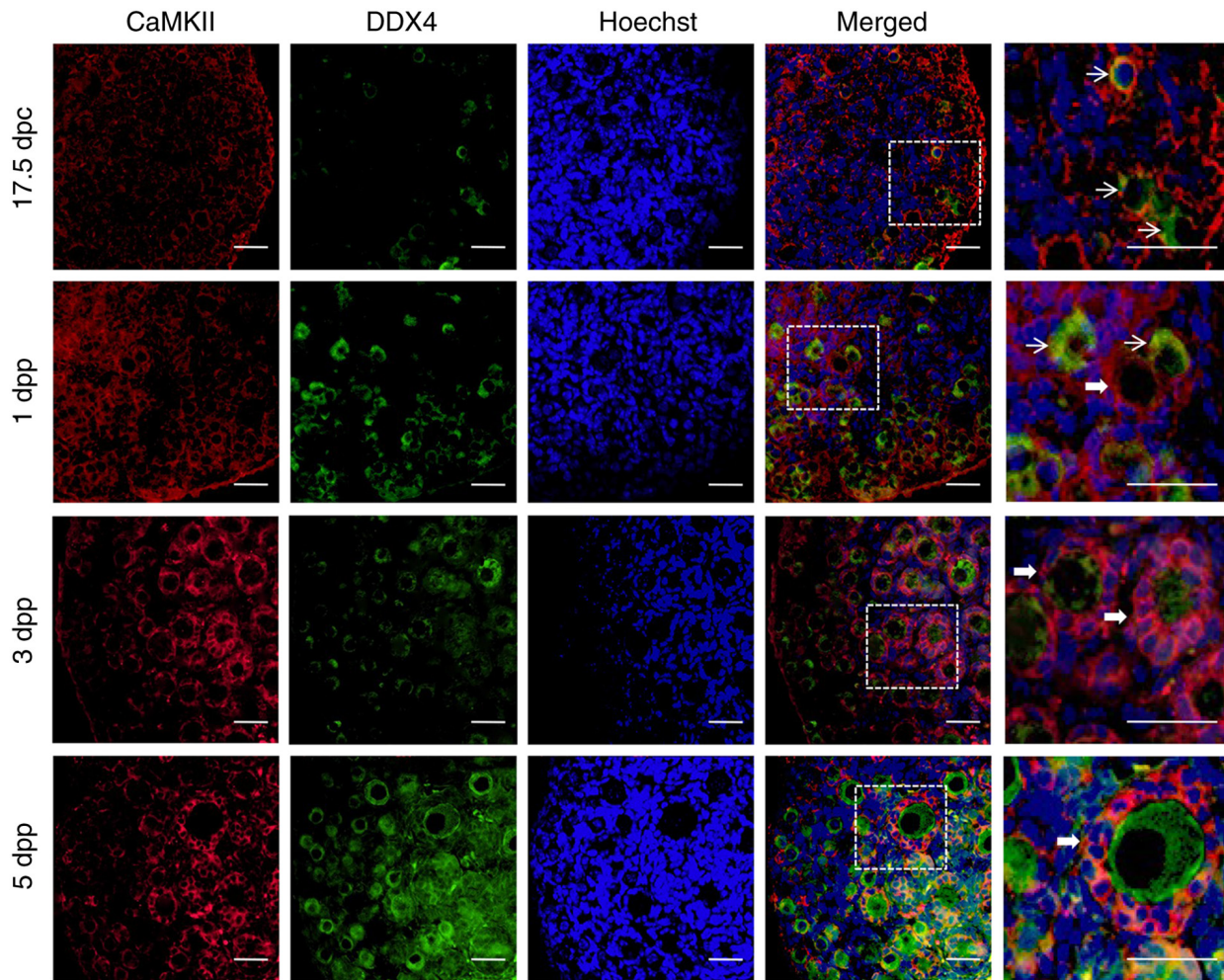
Figure 1. Expression pattern of CaMKII in the embryonic and neonatal mouse ovaries. The embryonic and neonatal mouse ovaries were stained for CaMKII (red) and the oocyte specific marker DDX4 (green) at the indicated time points. The nuclei were counter-stained using Hoechest (blue). CaMKII was mainly localized to the cytoplasm of granulosa cells in either primordial follicles or primary follicles. The thin arrows indicated primordial follicles, and the thick arrows indicated primary follicles. Scale bar, 40 μm (the first four columns) and 100 μm (the last column). CaMKII, calmodulin-dependent protein kinase II; DDX4, DEAD-box helicase 4; dpc, days post-coitus; dpp, days post-partum.
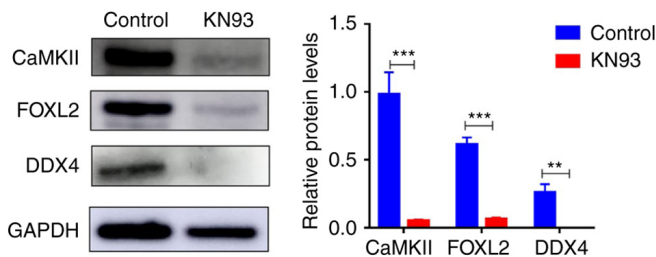

Figure 2. Western blotting for the 17.5 dpc ovaries that were cultured with or without KN93 for 4 days *in vitro*. The results revealed that KN93 significantly reduced the expression of CaMKII and the oocyte, granulosa cells specific marker DDX4 and FOXL2 in ovarian follicle. GAPDH was used as a loading control. The data are presented as the mean ± SD (n=3). **P<0.01, ***P<0.001. dpc, days post-coitus; CaMKII, calmodulin-dependent protein kinase II; DDX4, DEAD-box helicase 4; FOXL2, forkhead box L2.

Differentially expressed proteins affected by KN93 as revealed by proteomic techniques. To investigate the proteins affected by KN93 inhibition of CaMKII during ovarian development further, the ovaries of 17.5 dpc embryonic mice treated with KN93 and cultured for 4 days *in vitro* were collected. The protein samples were then detected by proteomics techniques. After detection, a total of 5,843 proteins were identified. Principal component analysis of the identified proteins indicated that the three samples of the KN93 treatment group and the three samples of the control group were clustered into different regions. This suggested that the genetic background of the three samples of the KN93 treatment group and the three samples of the control group showed good consistency. In addition, this suggested that the experimentally identified proteins could be used for further analysis (Fig. 4A). Among the 5,843 identified proteins, a total of 262 differentially expressed proteins were identified in the KN93 treatment group compared with the control group, including 168 proteins that were upregulated [$\log_2$ (fold-change)≥0.5 and P<0.01] and 94 proteins that were downregulated [$\log_2$ (fold-change) ≤0.5 and P<0.01] (Fig. 4B). Subsequently, 10 proteins from this list of 262 differentially expressed proteins were randomly selected for western blotting verification. It was revealed that two of the 10 proteins (Cyct and IGFBP3) did not concur with the proteomic results, which showed that there may be false positive results in proteomics, whilst the other eight proteins were consistent with the proteomic results and supported the high
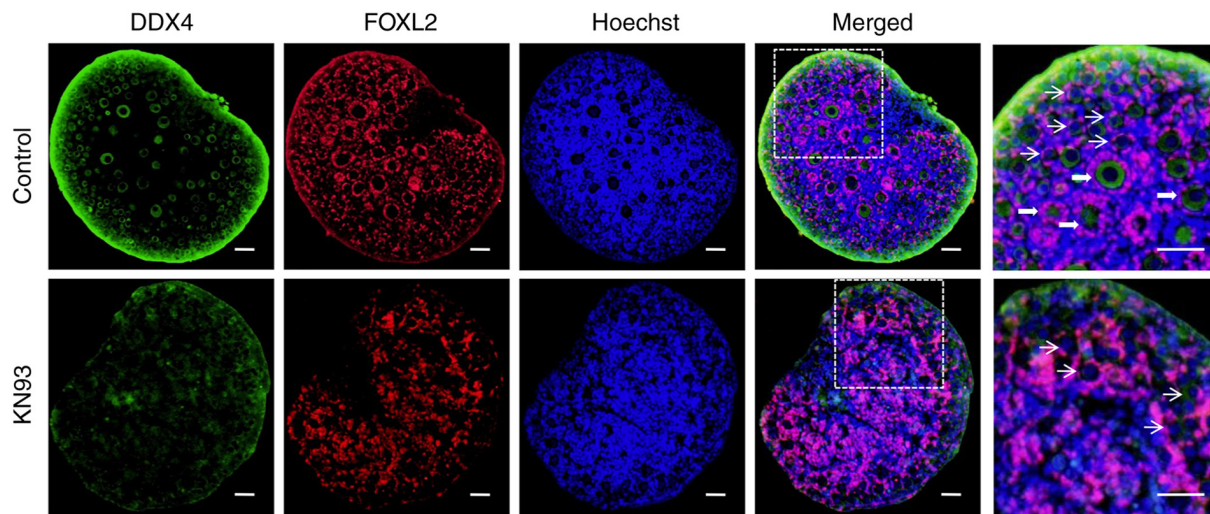
Figure 3. Immunofluorescence analysis for the 17.5 dpc ovaries that were *in vitro* cultured with or without KN93 for 4 days. Immunofluorescence detection results demonstrated that the development of follicles in KN93 treatment group was markedly inhibited compared with those in the respective controls. The ovaries were stained for the oocyte specific marker DDX4 (green) and the granulosa cells specific marker FOXL2 (red). The nuclei were counter-stained by Hoechest (blue). The thin arrows indicated primordial follicles, and the thick arrows indicated primary follicles. Scale bar, 20 μm (the first four columns) and 40 μm (the last column). dpc, days post-coitus; DDX4, DEAD-box helicase 4; FOXL2, forkhead box L2.

accuracy of this proteomic detection method (Fig. 4C and D). Taken together, these results suggested that KN93 inhibition of CaMKII could induce expression changes of various proteins during ovarian development.

Function analysis of differentially expressed proteins that are affected by KN93. To further investigate the biological functions and enrichment pathways of the differentially expressed proteins induced by KN93 during ovarian development, GO and KEGG enrichment analyses were performed for the obtained proteins in the present study. It was revealed that a number of cell molecules, cell components, biological processes or pathways associated with reproductive development, cell proliferation and differentiation or migration were enriched. In the GO terms of molecular function, 'retinol dehydrogenase activity', 'insulin-like growth factor binding', 'insulin-like growth factor II binding', 'iron ion binding' and 'zinc ion binding' were enriched (Fig. 5A). In the GO terms of cell components, 'insulin-like growth factor binding protein complex', 'growth factor complex', 'insulin-like growth factor ternary complex', 'autolysosome', 'intracellular ferritin complex' and 'ferritin complex' were enriched (Fig. 5B). In the GO terms of biological process, 'sterol biosynthetic process', 'renal system process', 'cholesterol biosynthetic process', 'secondary alcohol biosynthetic process', 'mast cell differentiation', 'mast cell proliferation' and 'mast cell migration' were enriched (Fig. 5C). Furthermore, important biological pathways that were enriched in terms of biological pathway mainly included 'steroid biosynthesis', 'p53 signaling pathway', 'metabolic pathways', 'retinol metabolism', 'cell adhesion molecules (CAMs)', and 'TGF-β signaling' pathway (Fig. 5D). Comprehensive analysis results revealed that KN93 inhibited CaMKII, which may serve an important role in reproductive regulation through these differentially expressed proteins. In particular, the differential proteins enriched in the biological pathways closely associated with reproductive development and metabolism may serve a key role in follicular development.

Potential mechanism of KN93 retarding follicular development. To further explore the potential mechanism of delaying follicular development after KN93 inhibits CaMKII, the present study extracted the main differentially expressed proteins enriched in the four biological pathways closely associated with reproductive development and metabolism obtained in the present study (Table I). It was revealed that 19 important differentially expressed proteins were enriched in the four biological pathways, among which all four differentially expressed proteins were downregulated whereas 15 differentially expressed proteins were upregulated (Table I). There are 15 differentially expressed proteins enriched in 'metabolic pathways', which included guanine deaminase, V-type proton ATPase subunit a, NADP-dependent steroid dehydrogenase-like (Nsdhl), Atp6v1c1, alcohol dehydrogenase 1 (Adh1), hydroxymethylglutaryl-CoA synthase 1 (Hmgcs1), fatty acid synthase (Fasn), α-L-iduronidase, dimethylallyltransferase (Fdps), DNA-directed RNA polymerase subunit, lanosterol synthase (Lss), N-acetylgalactosaminyltransferase 7, farnesyl-diphosphate farnesyltransferase 1 (Fdft1), NADH-ubiquinone oxidoreductase chain 5 and Lanosterol 14-alpha demethylase (Table I). Subsequently, four differentially expressed proteins were enriched in the 'p53 signaling pathway', including Igfbp3, Cyct, insulin-like growth factor-binding protein 5 (Igfbp5) and neuroserpin. In addition, four differential proteins were enriched in the 'steroid biosynthesis', including Nsdhl, Lss, Fdft1 and Cyp51a1. Only one differential protein was revealed to be enriched in 'retinol metabolism', which was Adh1. It was also revealed that Nsdhl, Lss, Fdft1 and Cyp51a1 were simultaneously enriched in 'steroid biosynthesis' and 'metabolic pathways'. Adh1 was enriched in both 'retinol metabolism' and 'metabolic pathways' (Table I). These results suggested that Nsdhl, Lss, Fdft1, Cyp51a1 and Adh1 were the key proteins affected by KN93.

Furthermore, the 19 important differentially expressed proteins in four biological pathways were incorporated into the interaction analysis. In total, seven of the 19 differentially
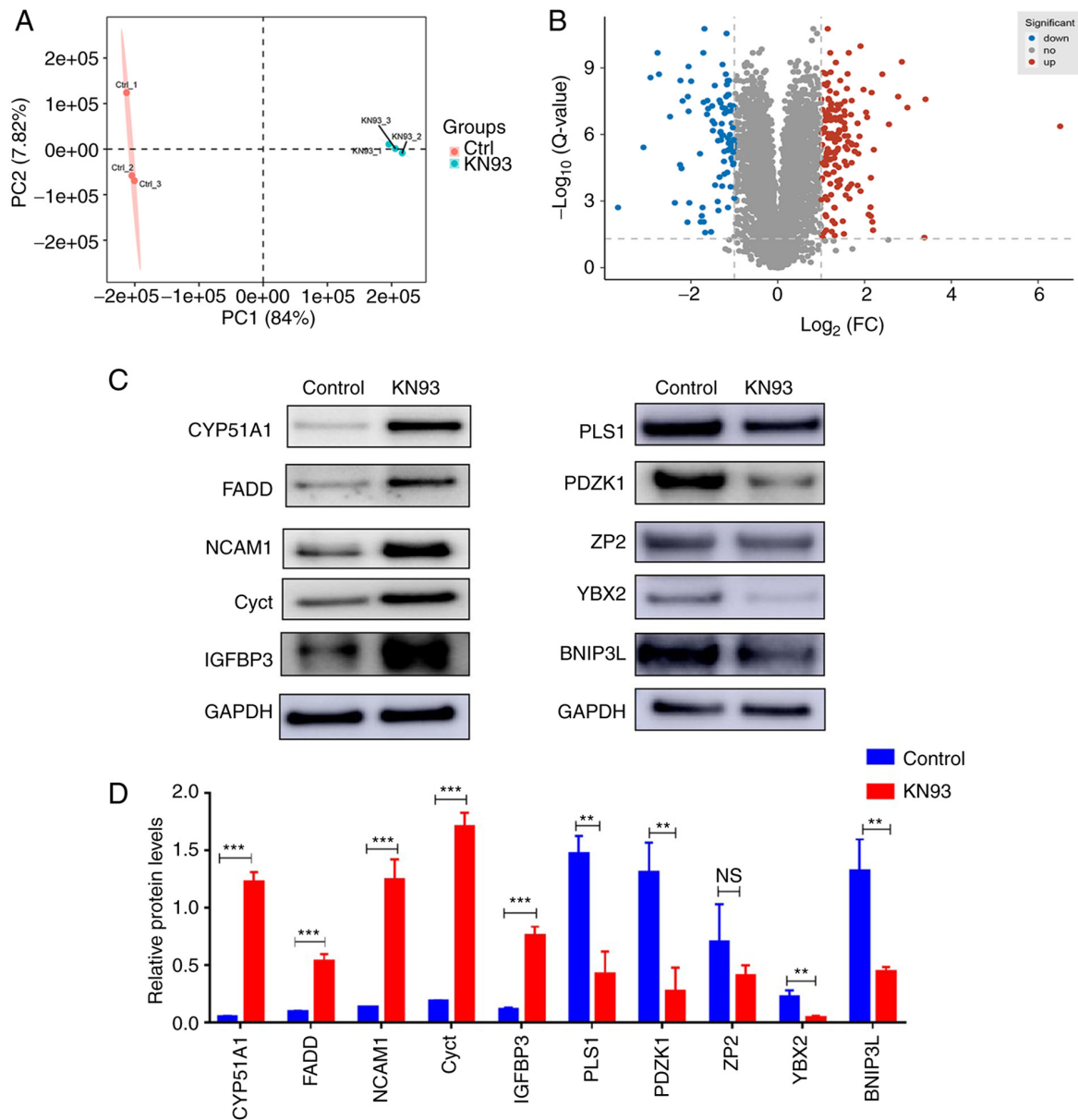
Figure 4. Proteomic techniques revealed differential proteins influenced by KN93. (A) Principal component analysis of the identified proteins in the KN93 treatment group and control group. Red and blue dots represent the KN93 treatment group and control group, respectively. (B) Volcano plot indicated the differential proteins between KN93 treatment group and control group. Red dots indicated significantly upregulated proteins with adjusted P-values <0.01, blue dots indicated significantly down-regulated proteins with adjusted P-values <0.01 and gray dots indicated non-significantly expressed proteins. (C) Differential proteins were verified by western blotting, which was then (D) quantified. GAPDH was used as a loading control. The data are presented as the mean ± SD (n=3). **P<0.01, ***P<0.001. NS, no significant difference; CYP51A1, cytochrome P450 family 51 family A member 1; FADD, fas-associated death domain; NCAM1, neural cell adhesion molecule 1; Cyct, cytochrome *c*, testis; IGFBP3, insulin-like growth factor binding protein 3; PLS1, plastin-1; PDZK1, PDZ domain-containing 1; ZP2, zona pellicida sperm-binding protein; YBX2, Y-box binding protein 2; BNIP3L, Bcl-2-interacting protein 3-like.

expressed proteins were revealed to have direct interactions, including Nsdhl, Lss, Fdft1, Cyp51, Hmgcs1, Fasn and Fdps (Fig. 6A). Combined with the analysis results aforementioned, it was revealed that among the seven differentially expressed proteins, Nsdhl, Lss, Fdft1 and Cyp51a1 were enriched in 'steroid biosynthesis', whilst Hmgcs1, Fasn and Fdps were enriched in 'metabolic pathways' (Table I; Fig. 6A). This result indicated that after KN93 inhibited CaMKII, it may be involved in the regulation of follicular development by affecting the expression levels of Nsdhl, Lss, Fdft1, Cyp51a1, Hmgcs1, Fasn and Fdps in 'steroid biosynthesis' and 'metabolic pathways'.

Based on these studies, the present study mapped the potential mechanism of KN93 inhibiting CaMKII and delaying follicular development further, where the possible regulatory mechanism was as follows: KN93 Inhibits CaMKII, which upregulates the expression levels of Nsdhl, Lss, Fdft1, Cyp51a1, Hmgcs1, Fasn and Fdps. This then downregulates the expression of the oocyte marker DDX4 and the granulosa cell marker FOXL2 in follicles, which ultimately slowed down the formation and activation of primordia follicles, leading to the delay in the follicle development (Fig. 6B).

Discussion

The ovary is the reproductive gland of female mammals, where the follicle forms the basic structural and functional
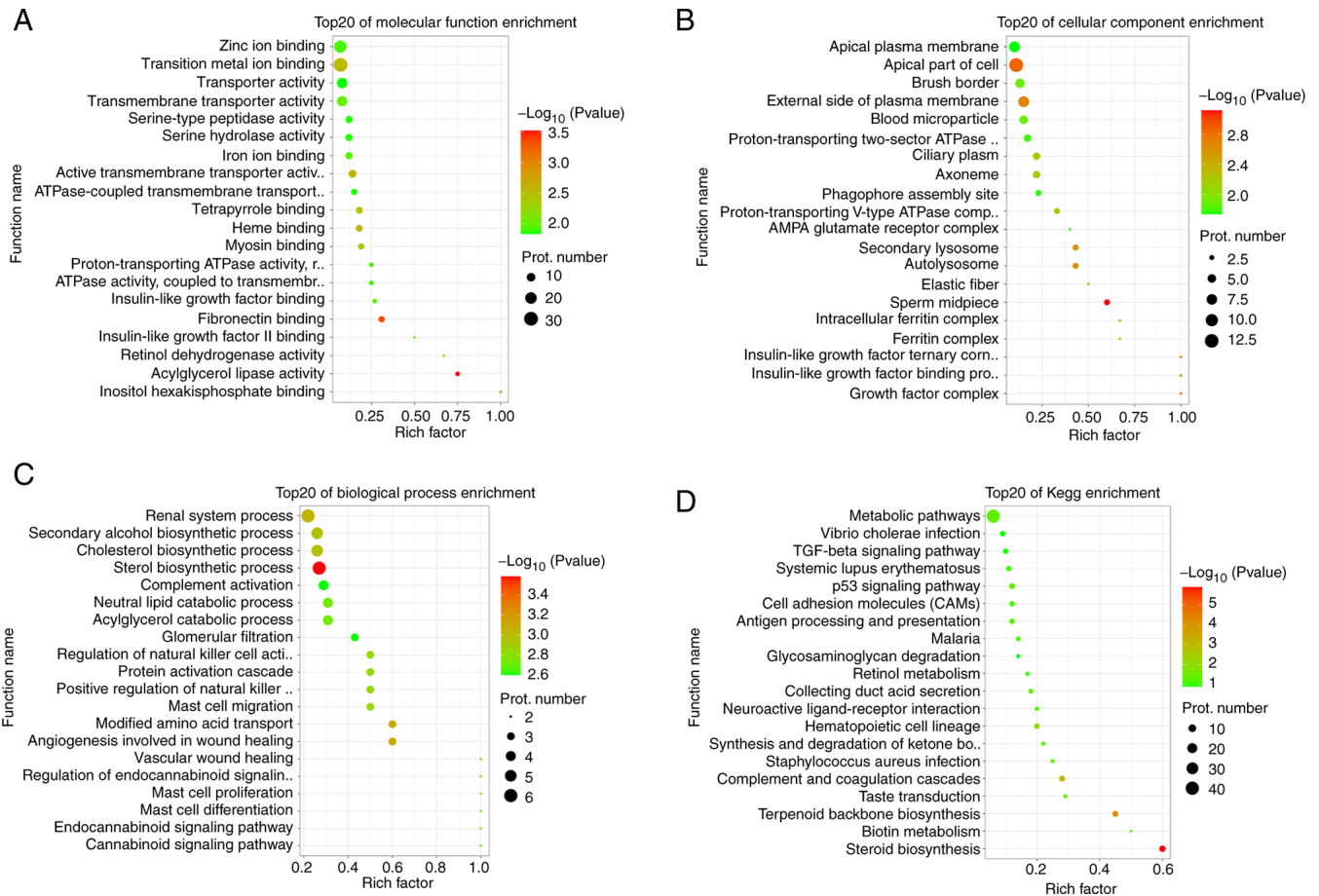
Figure 5. GO and KEGG enrichment analysis of differential proteins affected by KN93. (A) Enriched the top 20 GO terms in the (A) molecular function, (B) cell components and (C) biological process categories for the differential proteins. (D) Enriched the top 20 KEGG information for the differential proteins. GO, Gene Ontology; KEGG, Kyoto Encyclopedia of Genes and Genomes.

unit of the ovary (28). Follicles provide stable and controllable environments for oocyte development in addition to precisely controlling the mobilization of stored follicles, which can provide healthy oocytes for fertilization in a sustainable manner (29,30). By contrast, the somatic cells in the follicle can form a closely coordinated neuroendocrine system with the hypothalamus and the pituitary gland through endocrine and paracrine regulation, which regulates almost all physiological activities that occur during sexual reproduction (31). Follicular development begins with the formation of primordial follicles in the ovary. Formation of primordial follicles not only determines whether there are oocytes available for fertilization, establishment and maintenance of the primordial follicle reserve pool also directly determines the reproductive life span of female animals (32,33). It has been reported that in the ovaries of mice at 17.5 days of embryonic stage, only part of the cysts rupture to form a small number of primordial follicles (27). By contrast, in the ovaries of mice after birth, a large number of cysts rupture and primordial follicles are formed continuously, before formalizing the primordial follicle pool during the first 4-5 days after birth (34). Research has demonstrated that there are two different types of primordial follicles in the ovary. The first type is those in the medulla of the ovary, which are activated immediately after formation, whereas the second type is those in the cortex, which are gradually activated during the subsequent reproductive

years (35). Once the primordial follicle is activated, it begins further development into primary follicles and more advanced follicles (36).

The formation and activation of primordial follicles is a complex and delicate process that involves the co-ordination of molecular signaling pathways in the ovary. CaMKII is one such important regulatory molecule that has been demonstrated to serve a role in reproductive processes, such as oocyte and early embryonic development (18,19). However, the effects of CaMKII on follicular development remains unknown. In the present study, CaMKII was expressed in the ovaries of mice at embryonic stage 17.5 days and postnatal stage 1, 3 and 5 days, suggesting the possibility of CaMKII regulating follicular development. It was then revealed that CaMKII was mainly expressed in the cortical regions of the ovaries in mice at 17.5 days embryonic stage and those at 1-day postnatal stage. By contrast, it was mainly expressed in the primordial and primary follicles in the medulla region of the ovaries of neonatal mice at 3 and 5 days postnatal. These results suggested that CaMKII could activate primordial follicles. In addition, in the ovaries of newborn mice that are 3 and 5 days old, CaMKII was mainly expressed in the cytoplasm of granulosa cells in the primordial and primary follicles in the ovarian medulla region. Therefore, it was hypothesized that CaMKII could transform the flattened granulosa cells in the primordial follicles into cuboid granulosa cells, which could

Table I. Differential proteins enriched in the four key KEGG pathways closely related to reproductive development and metabolism.

Protein name	Accession	Description	KN93: Control state	Fold-change	Enrichment pathway
Igfbp3	P47878	Insulin-like growth factor-binding protein 3	Down	0.147	p53 signaling pathway
Cyct	P00015	Cytochrome c	Down	0.219	p53 signaling pathway
Gda	Q9R111	Guanine deaminase	Down	0.237	Metabolic pathways
Igfbp5	Q07079	Insulin-like growth factor-binding protein 5	Down	0.306	p53 signaling pathway
Tcirg1	Q9JHF5	V-type proton ATPase subunit a	Up	2.823	Metabolic pathways
Nsdhl	Q9R1J0	Sterol-4-alpha-carboxylate 3-dehydrogenase, decarboxylating	Up	2.915	Steroid biosynthesis, metabolic pathways
Atp6v1c1	Q9Z1G3	V-type proton ATPase subunit C 1	Up	2.916	Metabolic pathways
Adh1	P00329	Alcohol dehydrogenase 1	Up	3.002	Retinol metabolism, metabolic pathways
Serpini1	O35684	Neuroserpin	Up	3.026	p53 signaling pathway
Hmgcs1	Q8JZK9	Hydroxymethylglutaryl-CoA synthase, cytoplasmic	Up	3.048	Metabolic pathways
Fasn	P19096	Fatty acid synthase	Up	3.113	Metabolic pathways
Idua	Q8BLF6	α-L-iduronidase	Up	3.264	Metabolic pathways
Fdps	Q920E5	Farnesyl pyrophosphate synthase	Up	3.745	Metabolic pathways
Znrd1	G3UXD3	DNA-directed RNA polymerase subunit	Up	3.748	Metabolic pathways
Lss	Q8BLN5	Lanosterol synthase	Up	4.634	Steroid biosynthesis, Metabolic pathways
Galnt7	Q80VA0	N-acetylgalactosaminyltransferase 7	Up	5.906	Metabolic pathways
Fdft1	P53798	Squalene synthase	Up	7.25	Metabolic pathways, Steroid biosynthesis
Mtnd5	P03921	NADH-ubiquinone oxidoreductase chain 5	Up	10.587	Metabolic pathways
Cyp51a1	Q8K0C4	Lanosterol 14-alpha demethylase	Up	91.003	Steroid biosynthesis, Metabolic pathways

activate and develop into primary follicles. However, this hypothesis requires further experimental confirmation.

After the formation of the final primordial follicles pool, the periodic activation of primordial follicles will continuously deplete the number of primordial follicles, shortening the reproductive lifespan. Therefore, adequately regulating the speed of primordial follicle activation will prolong the reproductive life of the ovaries (5). A number of studies have previously reported that KN93 is a specific inhibitor of CaMKII that can regulate various physiological and pathological processes by specifically inhibiting CaMKII activity (20,21). However, to the best of our knowledge, it has not been previously reported whether KN93 can delay follicular development by inhibiting CaMKII.

In the present study, the ovaries of embryonic mice (17.5 dpc) treated with KN93 was observed following hematoxylin staining. It was revealed that a large proportion of primordial and primary follicles were observed in the deep cortex and medulla of the ovaries in the control group, but no such phenomenon was observed in the follicles in the KN93 group. These results suggested that KN93 could inhibit follicular development. Immunofluorescence detection also verified that the majority of the primordial and primary

follicles were localized to the deeper layers of the cortex and medulla in the ovaries in the control group. However, again no such phenomenon was observed in the KN93 treatment group, further confirming that KN93 exerted an inhibitory effect on follicular development. It has been previously reported that DDX4 and FOXL2 are markers of oocyte and granulosa cells in the follicles that can be used for determining the fate of follicular development (37,38). In the present study, immunofluorescence revealed that the fluorescence intensity of the oocyte marker DDX4 in follicles treated with KN93 was significantly weaker compared with that in the control group. By contrast, the fluorescence intensity of the granulosa cell marker FOXL2 in follicles was not altered compared with that in the control group. However, western blotting demonstrated that the expression of DDX4, CaMKII and FOXL2 in the ovaries after KN93 treatment group was significantly decreased. These results suggested that KN93 could reduce the expression levels of DDX4 and FOXL2 by inhibiting CaMKII to delay the development of follicles and activation of primordial follicles.

Although the results aforementioned reported that KN93 can inhibit CaMKII, reduce DDX4 and FOXL2 expression and delay follicular development, a more detailed mechanistic
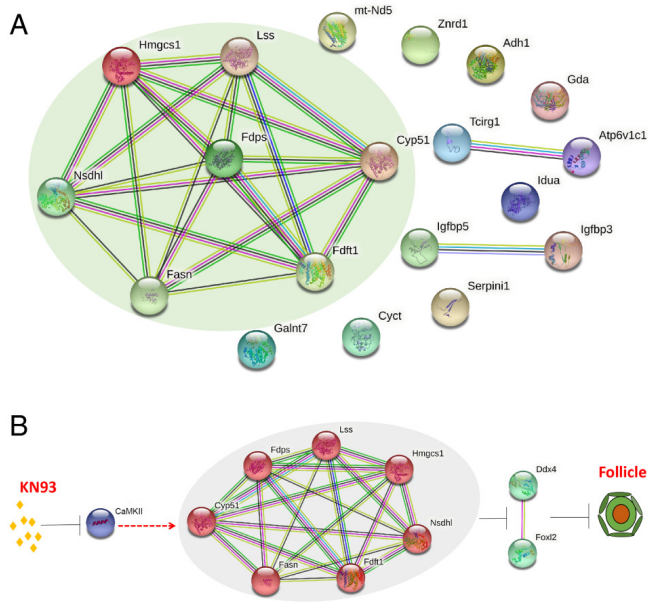
A

B

Figure 6. Analysis of potential mechanism for KN93 retarding ovarian follicle development. (A) Interaction analysis of differential proteins in four key KEGG enriched pathways. Nsdhl, Lss, Fdft1, Cyp51a1, Hmgcs1, Fasn and Fdps have direct interactions, which was marked through the pale green elliptic region. (B) Model of KN93 retarding follicular development. After CaMKII was inhibited by the inhibitor KN93, seven interacting proteins were upregulated (Nsdhl, Lss, Fdft1, Cyp51a1, Hmgcs1, Fasn and Fdps), then downregulated oocyte marker DDX4 and granulosa cell marker FOXL2 in follicles, ultimately slowing down primordial follicles formation and activation, thereby leaded to the delay of the ovarian follicle development. Nsdhl, NADP-dependent steroid dehydrogenase-like; Lss, lanosterol synthase; Fdft1, farnesyl-diphosphate farnesyltransferase; Cyp51a1, cytochrome P450 family 51 family A member 1; Hmgcs1, hydroxymethylglutaryl-CoA synthase 1; Fasn, fatty acid synthase; Fdps, dimethylallyltranstransferase; CaMKII, calmodulin-dependent protein kinase II; DDX4, DEAD-box helicase 4; FOXL2, forkhead box L2.

model underlying the effects of KN93 on follicular development remains to be fully elucidated. This is because after KN93 inhibits CaMKII activity, its downstream signaling target proteins remain unknown. To reveal the downstream target proteins that were altered after KN93 treatment, proteomics techniques were applied to measure these proteins *in vitro* in cultured ovaries treated with KN93. The expression levels of 262 proteins were demonstrated to be significantly altered between the KN93 treatment group and the control group. Furthermore, the expression of 10 differentially expressed proteins were measured by western blotting to validate the accuracy of the proteomics technique. Previous studies reported that a wide range of important signaling pathways are involved in the regulation of follicular development, including Notch, PI3K, KIT, TGF-β and JNK (9-13). In the present study, GO and KEGG enrichment analysis was performed on the 262 differentially expressed proteins obtained, which were mainly enriched in molecular and biological pathways associated with reproductive development, cell proliferation and differentiation or migration. In addition, four pathways were revealed to be closely associated reproductive development, namely 'steroid biosynthesis', 'p53 signaling pathway', 'retinol metabolism' and 'metabolic pathways'.

Discovery of the biological pathways aforementioned provided potentially important targets for studying the mechanism underlying the KN93-mediated delayed in follicular development. Therefore, the differentially expressed proteins were enriched in the four biological pathways of 'steroid biosynthesis', 'p53 signaling pathway', 'retinol metabolism and 'metabolic pathways'. Finally, 19 enriched differentially expressed proteins were obtained from these four biological pathways. Nevertheless, western blotting detection of these 19 differentially expressed proteins could not be carried out in the current study. This was because 10 differentially expressed proteins were randomly detected by proteomics using western blotting, which confirmed the reliability of the proteomic detection results in the study. Another important reason was that the ovarian materials of embryonic mice were limited. The ovaries required in the study were from the female embryos of 17.5 d pregnant mice and collected after *in vitro* culture for 4 days. The amount of proteins extracted from every 8-10 ovaries could only complete the detection of two proteins at a time. Therefore, to complete the western blotting analysis of the 19 differentially expressed proteins, enough ovaries must be collected, which would take several months or longer. Although these 19 differentially expressed proteins cannot be detected one by one in the present study, these 19 differentially expressed proteins will be studied one by one in the follow-up study.

In spite of this, for these 19 differential proteins, an interaction analysis was performed further, where among the 19 differentially expressed proteins, seven were upregulated, including Nsdhl, Lss, Fdft1, Cyp51a1, Hmgcs1, Fasn and Fdps, all of which interact which each other. The current results suggested that these seven differentially expressed proteins were the key downstream targets after CaMKII inhibition by KN93. A number of studies have revealed that Nsdhl, Lss, Fdft1, Cyp51a1, Hmgcs1, Fasn and Fdps can serve important roles in cholesterol synthesis by promoting this process (39-42). In addition, another study has also revealed that cholesterol synthesis is closely associated with ovarian reserve function, whereby patients with diminished ovarian reserves tended to exhibit significantly lower cholesterol metabolic levels compared with those with normal ovarian reserve (43). Based on these reports, it was hypothesized that these seven upregulated proteins may be involved in cholesterol synthesis during follicular development, thereby improving ovarian reserve function. In addition, the potential mechanism underlying the effects of KN93 inhibiting CaMKII on delaying follicular development can be summarized as follows: KN93 Inhibits CaMKII, which upregulates the expression of Nsdhl, Lss, Fdft1, Cyp51a1, Hmgcs1, Fasn and Fdps to promote cholesterol synthesis. This then downregulates the expression of the oocyte marker DDX4 and the granulosa cell marker FOXL2 in follicles, leading to the delay in the formation and activation of primordial follicles. Although the potential mechanism of KN93 inhibiting CaMKII in delaying follicular development has been suggested by data from the present study, its authenticity require validation in further studies.

To the best of our knowledge, the present study demonstrated for the first time that KN93, an inhibitor of CaMKII, can directly delay follicular development in mouse ovaries and reveal its underlying regulatory mechanism. Therefore, these results suggest that KN93 may be a promising therapeutic agent for delaying follicular development, thereby prolonging the reproductive life of female individuals in the future.

Availability of data and materials

The mass spectrometry proteomics data have been deposited to the ProteomeXchange Consortium (http://proteomecentral.proteomexchange.org) via the iProX partner repository with the dataset identifier PXD035136. The datasets used and/or analyzed during the current study are available from the corresponding author on reasonable request.

Authors' contributions

JY, XX and YM performed the experiments. YY and CW analyzed the data. GX conducted literature search and analyzed the data. XD analyzed and interpreted the immunofluorescence images. XL and XD can confirm the authenticity of all the raw data. XL designed the study. All authors read and approved the final manuscript.

Ethics approval and consent to participate

All experiments were reviewed and approved by the Animal Ethical and Welfare Committee of Ningxia University (approval no. IACUC-NDLAC-2020019).

Patient consent for publication

Not applicable.

Competing interests

The authors declare that they have no competing interests.

References

1. Shah JS, Sabouni R, Vaught KCC, Owen CM, Albertini DF and Segars JH: Biomechanics and mechanical signaling in the ovary: A systematic review. J Assist Reprod Genet 35: 1135-1148, 2018.
2. Green LJ and Shikanov A: In vitro culture methods of preantral follicles. Theriogenology 86: 229-238, 2016.
3. West ER, Shea LD and Woodruff TK: Engineering the follicle microenvironment. Semin Reprod Med 25: 287-299, 2007.
4. Simon LE, Kumar TR and Duncan FE: In vitro ovarian follicle growth: A comprehensive analysis of key protocol variables. Biol Reprod 103: 455-470, 2020.
5. Zhang T, He M, Zhao L, Qin S, Zhu Z, Du X, Zhou B, Yang Y, Liu X, Xia G, et al: HDAC6 regulates primordial follicle activation through mTOR signaling pathway. Cell Death Dis 12: 559, 2021.
6. Guo R and Pankhurst MW: Accelerated ovarian reserve depletion in female anti Müllerian hormone knockout mice has no effect on lifetime fertility†. Biol Reprod 102: 915-922, 2020.
7. Chen J, Liu W, Lee KF, Liu K, Wong BPC and Yeung WSB: Overexpression of Lin28a induces a primary ovarian insufficiency phenotype via facilitation of primordial follicle activation in mice. Mole Cell Endocrinol 539: 111460, 2022.
8. Zhang J, Yan L, Wang Y, Zhang S, Xu X, Dai Y, Zhao S, Li Z, Zhang Y, Xia G, et al: In vivo and in vitro activation of dormant primordial follicles by EGF treatment in mouse and human. Clin Transl Med 10: e182, 2020.
9. Xu J and Gridley T: Notch2 is required in somatic cells for breakdown of ovarian germ-cell nests and formation of primordial follicles. BMC Biol 11: 13, 2013.
10. Zhang H and Liu K: Cellular and molecular regulation of the activation of mammalian primordial follicles: Somatic cells initiate follicle activation in adulthood. Hum Reprod Update 21: 779-786, 2015.
11. Huang K, Wang Y, Zhang T, He M, Sun G, Wen J, Yan H, Cai H, Yong C, Xia G and Wang C: JAK signaling regulates germline cyst breakdown and primordial follicle formation in mice. Biol Open 7: bio029470, 2018.
12. Wang ZP, Mu XY, Guo M, Wang YJ, Teng Z, Mao GP, Niu WB, Feng LZ, Zhao LH and Xia GL: Transforming growth factor-β signaling participates in the maintenance of the primordial follicle pool in the mouse ovary. J Biol Chem 289: 8299-8311, 2014.
13. Komatsu K and Masubuchi S: Increased supply from blood vessels promotes the activation of dormant primordial follicles in mouse ovaries. J Reprod Dev 66: 105-113, 2020.
14. Hea Q, Chengb J and Wang Y: Chronic CaMKII inhibition reverses cardiac function and cardiac reserve in HF mice. Life Sci 219: 122-128, 2019.
15. Zhu Q, Hao L, Shen Q, Pan J, Liu W, Gong W, Hu L, Xiao W, Wang M, Liu X, et al: CaMK II Inhibition attenuates ROS dependent necroptosis in acinar cells and protects against acute pancreatitis in mice. Oxid Med Cell Longev 17: 4187398, 2021.
16. Altobelli GG, Van Noorden S, Cimini D, Illario M, Sorriento D and Cimini V: Calcium/calmodulin-dependent kinases can regulate the TSH expression in the rat pituitary. J Endocrinol Invest 44: 2387-2394, 2021.
17. Hoch B, Haase H, Schulze W, Hagemann D, Morano I, Krause EG and Karczewski P: Differentiation-dependent expression of cardiac delta-CaMKII isoforms. J Cell Biochem 68: 259-268, 1998.
18. Medvedev S, Stein P and Schultz RM: Specificity of calcium/calmodulin-dependent protein kinases in mouse egg activation. Cell Cycle 13: 1482-1488, 2014.
19. Jin XL and O'Neill C: The presence and activation of two essential transcription factors (cAMP response element-binding protein and cAMP-dependent transcription factor ATF1) in the two-cell mouse embryo. Biol Reprod 82: 459-468, 2010.
20. Wang J, Xu X, Jia W, Zhao D, Boczek T, Gao Q, Wang Q, Fu Y, He M, Shi R, et al: Calcium-/calmodulin-dependent protein kinase II (CaMKII) inhibition induces learning and memory impairment and apoptosis. Oxid Med Cell Longev 2021: 4635054, 2021.
21. Johnson CN, Pattanayek R, Potet F, Rebbeck RT, Blackwell DJ, Nikolaienko R, Sequeira V, Meur RL, Radwański PB Davis JP, et al: The CaMKII inhibitor KN93-calmodulin interaction and implications for calmodulin tuning of NaV1.5 and RyR2 function. Cell Calcium 82: 102063, 2019.
22. Yang X, Wu N, Song L and Liu Z: Intrastriatal injections of KN-93 ameliorates levodopa-induced dyskinesia in a rat model of Parkinson's disease. Neuropsychiatr Dis Treat 9: 1213-1220, 2013.
23. Liu Y, Liang Y, Hou B, Liu M, Yang X, Liu C, Zhang J, Zhang W, Ma Z and Gu X: The inhibitor of calcium/calmodulin-dependent protein kinase II KN93 attenuates bone cancer pain via inhibition of KIF17/NR2B trafficking in mice. Pharmacol Biochem Behav 124: 19-26, 2014.
24. Edvinsson L, Povlsen GK, Ahnstedt H and Waldsee R: CaMKII inhibition with KN93 attenuates endothelin and serotonin receptor-mediated vasoconstriction and prevents subarachnoid hemorrhage-induced deficits in sensorimotor function. J Neuroinflammation 11: 207, 2014.
25. Chen W, An P, Quan XZ, Zhang J, Zhou ZY, Zou LP and Luo HS: Ca²⁺/calmodulin-dependent protein kinase II regulates colon cancer proliferation and migration via ERK1/2 and p38 pathways. World J Gastroenterol 23: 6111-6118, 2017.
26. Shin H, Han C, Labuz ML, Kim J, Kim J, Cho S, Gho YS, Takayama S and Parka J: High-yield isolation of extracellular vesicles using aqueous two-phase system. Sci Rep 5: 13103, 2015.

27. He Y, Chen Q, Dai J, Cui Y, Zhang C, Wen X, Li J, Xiao Y, Peng X, Liu M, *et al*: Single-cell RNA-Seq reveals a highly coordinated transcriptional program in mouse germ cells during primordial follicle formation. Aging Cell 20: e13424, 2021.
28. Bazot M, Robert Y, Mestdagh P, Boudghène F and Rocourt N: Ovarian functional disorders. J Radiol 81: 1801-1818, 2000 (In French).
29. Fortune JE, Rivera GM and Yang MY: Follicular development: The role of the follicular microenvironment in selection of the dominant follicle. Anim Reprod Sci 82: 109-126, 2004.
30. Sun L, Chen L, Jiang Y, Zhao Y, Wang F, Zheng X, Li C and Zhou X: Metabolomic profiling of ovary in mice treated with FSH using ultra performance liquid chromatography/mass spectrometry. Biosci Rep 38: BSR20180965, 2018.
31. Hirshfield AN: Development of follicles in the mammalian ovary. Int Rev Cytol 124: 43-101, 1991.
32. Li T, Liu X, Gong X, Qiukai E, Zhang X and Zhang X: microRNA 92b-3p regulate primordial follicle assembly by targeting TSC1 in neonatal mouse ovaries. Cell Cycle 18: 824-833, 2019.
33. Wang J, Ge W, Zhai QY, Liu JC, Sun XW, Liu WX, Li L, Lei CZ, Dyce PW, De Felici M and Shen W: Single-cell transcriptome landscape of ovarian cells during primordial follicle assembly in mice. PLoS Biol 18: e3001025, 2020.
34. Bristol-Gould SK, Kreeger PK, Selkirk CG, Kilen SM, Cook RW, Kipp JL, Shea LD, Mayo KE and Woodruff TE: Postnatal regulation of germ cells by activin: The establishment of the initial follicle pool. Dev Biol 298: 132-148, 2006.
35. Yin H, Kristensen SG, Jiang H, Rasmussen A and Andersen CY: Survival and growth of isolated pre-antral follicles from human ovarian medulla tissue during long-term 3D culture. Hum Reprod 31: 1531-1539, 2016.
36. Zhai J, Zhang J, Zhang L, Liu X, Deng W, Wang H, Zhang Z, Liu W, Chen B, Wu C, *et al*: Autotransplantation of the ovarian cortex after in vitro activation for infertility treatment: A shortened procedure. Hum Reprod 36: 2134-2147, 2021.
37. Song K, Ma W, Huang C, Ding J, Cui D and Zhang M: expression pattern of mouse vasa homologue (MVH) in the ovaries of C57BL/6 female mice. Med Sci Monit 22: 2656-2663, 2016.
38. Georges A, Auguste A, Bessière L, Vanet A, Todeschini AL and Veitia RA: FOXL2: A central transcription factor of the ovary. J Mol Endocrinol 52: R17-R33, 2013.
39. Su Y, Sugiura K, Wigglesworth K, O'Brien MJ, Affourtit JP, Pangas SA, Matzuk MM, and Eppig JJ: Oocyte regulation of metabolic cooperativity between mouse cumulus cells and oocytes: BMP15 and GDF9 control cholesterol biosynthesis in cumulus cells. Development 135: 111-121, 2008.
40. Ershov P, Kaluzhskiy L, Mezentsev Y, Yablokov E, Gnedenko O and Ivanov A: Enzymes in the cholesterol synthesis pathway: Interactomics in the cancer context. Biomedicines 9: 895, 2021.
41. Nakamura T, Iwase A, Bayasula B, Nagatomo Y, Kondo M, Nakahara T, Takikawa S, Goto M, Kotani T, Kiyono T and Kikkawa F: CYP51A1 induced by growth differentiation factor 9 and follicle-stimulating hormone in granulosa cells is a possible predictor for unfertilization. Reprod Sci 22: 377-384, 2015.
42. Jin Y, Chen Z, Dong J, Wang B, Fan S, Yang X and Cui M: SREBP1/FASN/cholesterol axis facilitates radioresistance in colorectal cancer. FEBS Open Bio 11: 1343-1352, 2021.
43. Yang X, Zhao Z, Fan Q, Li H, Liu LZC and Liang X: Cholesterol metabolism is decreased in patients with diminished ovarian reserve. Reprod Biomed Online 44: 185-192, 2022.